CHARACTERIZATION OF POLYCARBONATE FOAM STRUCTURE PREPARED BY ONE-STEP SC-CO_2 DISSOLUTION PROCESS

Gabriel Gedler, Marcelo Antunes, Vera Realinho and José I. Velasco.
Centre Català del Plàstic, Departament de Ciència dels Materials i Enginyeria Metal·lúrgica, Universitat Politècnica de Catalunya, BarcelonaTech. C/Colom 114.08222 Terrassa.Barcelona, Spain.

Abstract

In this communication, polycarbonate foams were prepared by a supercritical CO_2 dissolution one-step batch foaming process. Firstly, CO_2 diffusion behavior in polycarbonate was studied by means of desorption experiments. The cellular structure of foams prepared under different foaming conditions was characterized through scanning electron microscopy. Different foaming temperatures as well as CO_2 saturation pressures and times were applied. The foams displayed typical closed-cell structures with cell densities ranging from 3×10^5 to 6×10^6 cells/cm^3 and cell average sizes from around 70 to 150 μm. Analysis by X-ray diffraction and differential scanning calorimetry seemed to suggest that slight crystallization took place because of the plasticizing effect of CO_2 during saturation and foaming. Thermogravimetric analysis showed a higher thermal stability of the foams when compared to the compact polymer.

The preliminary results shown in this work suggest the possibility of developing lightweight polycarbonate components with improved specific thermal properties through carefully controlling the foaming parameters.

Introduction

Polycarbonate (PC) is one of the most used engineering plastics and polymeric foams are currently used in industrial applications where lightness is a key factor [1]. The final properties of these foams depend on their cellular structure, which includes parameters such as the average cell size and size distribution, cell volume fraction and cell arrangement within the matrix [2]. Nevertheless, the use of polymer foams is somewhat limited due to the inherent reduction of their mechanical properties with foaming when compared to the unfoamed base material. These foams are known for displaying better specific properties when cell sizes are reduced to a micrometer scale, hence having the potential to significantly alter the way plastics are employed in a wide variety of applications [3]. One of the most common microcellular foaming processes uses a physical blowing agent that creates an evenly distributed micrometric-sized closed cell structure, which significantly improves the mechanical properties compared to more heterogeneous or open cell structures [4]. Supercritical carbon dioxide (sc-CO_2) is one of the most favorable foaming agents due to its combination of chemical inertness, non-flammability and mild supercritical conditions (T_c = 31 ºC, P_c = 7.38 MPa) [5], also being environmentally benign [6]. One of the advantages of using physical blowing agents is that cell structure may be controlled through the processing temperature and pressure. Nevertheless, in order to optimize the foam properties, an overall understanding of the gas diffusion and the nucleation and growth mechanisms is required [2]. The influence of the foaming conditions has lately been considered, mainly focused in obtaining high performance foams by means of decreasing cell size [7].

It is known that some polymers, when processed with CO_2 undergo kinetically favorable configuration rearrangement of polymer chains, hence forming crystalline structures. For polycarbonate, the crystallization is very slow due to its inherent chain rigidity, which retards chain diffusion and ultimately inhibits crystallization at commonly used industrial processing conditions [8]. Thus, different strategies such as the addition of organic solvents [9], vapors [10], low melting point polymers [11], supercritical carbon dioxide [12], vapor-grown carbon fibres [13] or nano-sized fillers [14] have been used to induce the crystallization of polycarbonate. Therefore, foaming using sc-CO_2 could have a significant effect in the possible crystallization of PC.

The purpose of this study was to prepare polycarbonate foams through a physical sc-CO_2 one-step batch foaming process and to characterize them in terms of the developed cellular structure morphology and observe the effect of the foaming process on the crystallinity of polycarbonate.

Materials and foaming

Polycarbonate (Lexan-123R-PC, supplied by Sabic), with a density of 1.2 g/cm^3 and MFI of 17.5 dg/min, measured at 300 ºC and 1.2 kg, was melt-mixed using a Brabender Plasti-Corder internal mixer.

Firstly, the PC pellets were slowly introduced in the internal mixer at a temperature of 180 ºC using a rotating speed of 30 rpm during 2 min. Then the rotating speed was increased to 60 rpm and 120 rpm for 1 and 3 min,

respectively. The material was cooled at room temperature, grinded and compression-moulded at 220 ºC and 4.5 MPa (45 bar) in a hot-plate press (IQAP LAP PL-15) to discs with a thickness of 3.5 mm and diameter of 74 mm in 3 steps. In the first step the upper hot plate was used to soften the material at a temperature of 220 ºC. The second step consisted in allowing air to escape the material by pulsating the upper plate in an up and down motion. The pressure applied from the upper plate was 4.5 MPa (45 bar) at a temperature of 220 ºC during 1.5 min. For the third step the material was continuously compressed for 1 min at 220 ºC and 4.5 MPa. Lastly, the mould with the sample still inside was left to cool for 15 min in the cooling station of the press applying a constant pressure of 4.5 MPa. The discs used in the CO_2 desorption measurements were prepared by mechanically reducing the disc diameter to a typical value of 40 mm.

The resulting compression-molded discs were used to prepare the foams by sc-CO_2 dissolution using a one-step batch process that consisted in saturating the discs with CO_2 inside the high pressure vessel at pressures varying from 13 to 22 MPa during time periods between 0 and 40 min. The values of the saturation/foaming temperature varied between 200 and 213 ºC, and foaming was done in one-step by applying a sudden pressure drop, keeping residual pressure of 1 MPa (10 bar), as it was the optimal residual pressure to attain spherical-like cellular structures (AR = 1), found in one of our previous work [15].

Measurements and testing

In order to determine both the solubility and diffusion coefficient of CO_2 in the polycarbonate, CO_2 desorption measurements were carried out. Samples were introduced in the high pressure vessel and heated up to 210 ºC at a CO_2 pressure of 16 MPa. After reaching the saturation conditions, the samples were cooled to 40 ºC and the vessel was fully decompressed. Next, the saturated samples were removed from the vessel and quickly transferred to a digital balance (Mettler Toledo PB303 DeltaRange, with a sensitivity of 1 mg) at room temperature and atmospheric pressure, in order to record the CO_2 mass loss as a function of desorption time.

The maximum concentration of CO_2 in the samples after full decompression (M_o) was calculated by extrapolating to zero desorption time using the initial slope method [16]. Assuming one-dimensional diffusion in a plane sheet, the CO_2 desorption diffusion coefficient (D_d) was determined by plotting M_t/M_o vs. t/l^2, where M_t is the CO_2 concentration at time t and l is the thickness of the sample, according to the following equation [17]:

$$\frac{M_t}{M_t} = 1 - \frac{8}{\pi^2} exp\left(\frac{-D_d t}{l^2}\right) \quad (1)$$

The cellular structure of the foams was analyzed from scanning electron microscopy images obtained using a JEOL JSM-5610 microscope applying a voltage of 15 kV and a working distance of 30 mm. Samples were previously prepared by fracturing at room temperature and depositing a thin layer of gold onto their surface in argon atmosphere using a BAL-TEC SCD005 Sputter Coater.

The average cell sizes (ϕ) in the vertical (ϕ_{VD}) and width (ϕ_{WD}) foaming directions were measured using the intercept counting method [18]. The cell aspect ratio (AR) was determined by dividing the value of the average cell size in the vertical direction by that measured in the horizontal one ($AR = \phi_{VD}/\phi_{WD}$). The cell density (N_f) was calculated using the following equation [19]:

$$N_f = \left(\frac{n}{A}\right)^{\frac{3}{2}} \left(\frac{\rho_s}{\rho_f}\right) \quad (2)$$

WAXS was carried out using a Panalytical diffractometer using Cu Kα radiation with a λ= 1.54 Å operating at 40 KV and 40 mA at room temperature. Scans were taken from 2 to 60 deg (2θ) using a calibration with an accuracy of 0.02 deg. The crystallinity percentage (*X*c) was determined taking into consideration the WAXS patterns according to:

$$X_c(\%) = \frac{A_c}{A_c + A_a} 100 \quad (3)$$

where A_c corresponds to the crystalline peak area and A_a to the amorphous halo area.

DSC was carried out using a Perkin Elmer, Pyris 1 model with a glycol-based Perkin Elmer Intracooler IIP calorimeter at a heating rate of 10 ºC/min from 30 to 300 ºC using samples weighting around 4.0 mg. The glass transition temperature (T_g) of the unfoamed and foamed polycarbonate was determined using the inflection point heat capacity method. The melting temperature (T_m) was determined as the maximum temperature of the melting peak appearing in the melting endotherm, while the heat of fusion (ΔH) was obtained by direct integration of the peak. The crystallinity percentage (X_c) was determined according to:

$$X_c = \frac{\Delta H_m}{\Delta H_m^0 w_p} 100 \quad (4)$$

where w_p is the weight fraction of PC, ΔH_m is the melting enthalpy of the sample obtained by DSC and ΔH_m^o is the theoretical 100 % crystalline PC melting enthalpy (147.79 J/g)[17]).

Thermogravimetric analysis was performed in a TGA/DSC 1 Mettler Toledo Star System analyzer by heating samples of around 10.0 mg from 30 to 1000 ºC at a heating rate of 10 ºC/min under both nitrogen (constant 30 ml/min N_2 flow) and air atmospheres (constant 60 ml/min air flow). The temperatures corresponding to mass losses of 1, 5 and 50%, as well as the mass of the final residue obtained at 1000 ºC, were reported for the unfoamed and foamed polycarbonate.

Results and discussion

CO_2 diffusion coefficient from desorption measurements

The maximum concentration of CO_2 dissolved into PC was calculated by extrapolating to zero desorption time from the desorption measurements show in figure 1, finding a value of 42.6 mg CO_2/g material. As a result, the calculated diffusion coefficient (D_d) was 4.45×10^{-12} m^2/s obtained from the slope of figure 1(see graph embedded in Figure 1).

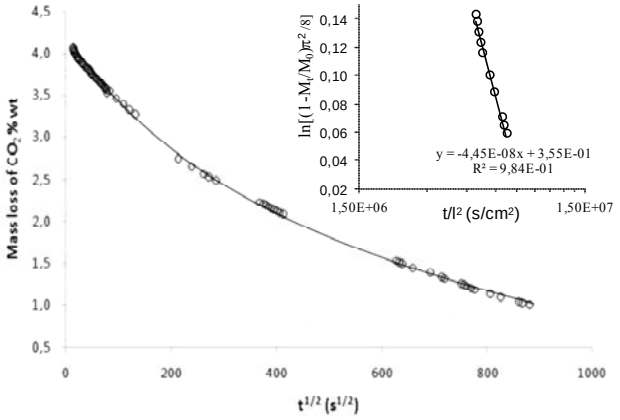

Figure 1. Results from the desorption study.

This value of the CO_2 diffusion coefficient in PC was found to be comparable to others presented in the literature, where D_d was found to be within 2.55×10^{-11} and 4.60×10^{-12} m^2/s [20] or between 1.55×10^{-12} and 6.93×10^{-12} m^2/s [21]. This result might suggest that the different in the values could be related to the degree of resistance that the CO_2 may have when desorbing the material, which could be related to the degree of crystallinity.

Cellular structure of PC foams

Polycarbonate foams (PC-f) were characterized by analyzing several scanning electron micrographs at different magnifications for each foam (typical SEM micrographs are displayed in Figure 2). The average cell size was determined for each foam obtained at a given saturation/foaming temperature, resulting in a variation in the cell density value from 1.04×10^6 to 2.70×10^6 cells/cm^3. The relative densities of the PC-f ranged from 0.33 to 0.46. As expected, a characteristic homogeneous microcellular structure was obtained due to the CO_2 saturation and sudden depressurization applied during foaming, with both the sudden pressure drop and time at saturation influencing the cell nucleation stage.

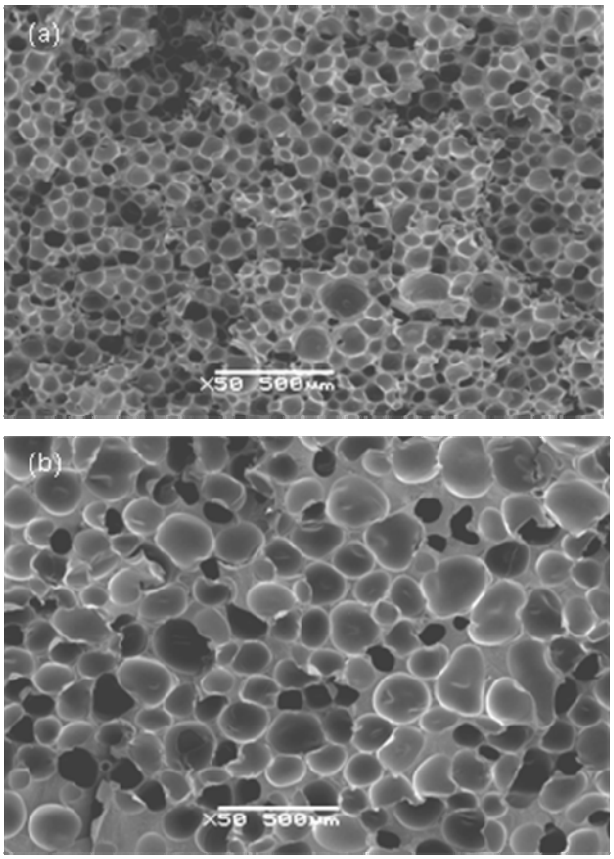

Figure 2. Typical SEM micrographs of the PC foams obtained at different saturation/foaming temperatures: (a) 200 ºC and (b) 205 ºC.

Figure 3 shows how cell size was clearly affected by the saturation/foaming temperature. Generally speaking, cell size increased from 70 to 160 μm with increasing the saturation/foaming temperature from 200 to 213 ºC, attributed to a higher concentration of CO_2 dissolved in the material. Decreasing the foaming temperature restricted cell growth and resulted in foams with higher

relative densities. During the sudden depressurization stage, the temperature of the growing sample decreased quickly, mainly due to the adiabatic expansion of the gas, and in a minor way due to the water cooling system of the vessel. Hence, this behavior can be explained by a faster rigidization of the softened material foamed at a lower temperature during the depressurization stage, reaching faster the glass transition temperature of the polymer than the samples foamed at higher temperatures.

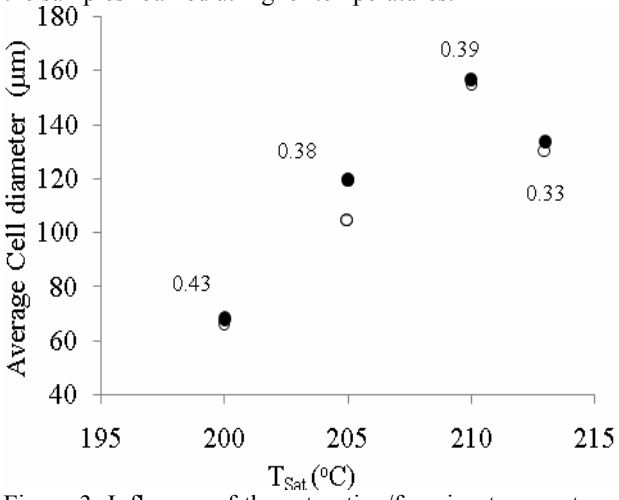

Figure 3. Influence of the saturation/foaming temperature on the average cell size of the PC foams. Hollow symbols: ϕ_{VD}; filled symbols: ϕ_{WD}. The relative density is indicated.

Crystalline structure of PC foams

WAXS measurements revealed the presence of a crystalline structure with diffractograms characterized by one strong peak at 2θ = 17.3º, corresponding to the monoclinic lattice reflections of (020),($\bar{2}$01) of crystalline PC [22]. Figure 4a shows a broad amorphous halo for the unfoamed PC and the presence of crystallization in the PC-f. The PC-f samples presented different degrees of crystallization depending on the process parameters used during the saturation/foaming stage. The increment of the temperature, pressure and time at CO_2 saturation conditions suggests the increment of crystallinity of the samples.

Table 1. Values of crystallinity calculated by WAXS and DSC.

Sample	Relative density	χ_c (%) by WAXS	χ_c (%) by DSC
PC	1	0	0
PC-s	1	0	0.2
1PC-f	0.43	0.95	0
2PC-f	0.46	0	0.57
3PC-f	0.38	0.51	0.97
4PC-f	0.39	1.04	0.45
5PC-f	0.33	0	0

It has been mentioned in the literature that crystalline PC may show other reflections as the (213) for a 2θ of 21.1º and the reflection of ($\bar{2}$22),(303),(223) around a 2θ of 25.3º [22, 23]. For the PC-f samples these aforementioned reflections were not very strong. However, very weak signals were noticed around 2θ = 20º and 2θ =25.3º, similar to the values found in the literature.

The differential scanning calorimetry analysis also showed that the PC-f samples obtained by sc-CO_2 dissolution presented melting peaks corresponding to PC crystallization (Figure 4(b)). The DSC study suggests that the saturation/foaming pressure might have an important effect on the crystallinity of the polycarbonate foams, showing a higher crystallinity for foams prepared with higher foaming pressures. Table 1 resumes the results of crystallinity calculated from WAXS and DSC measurements.

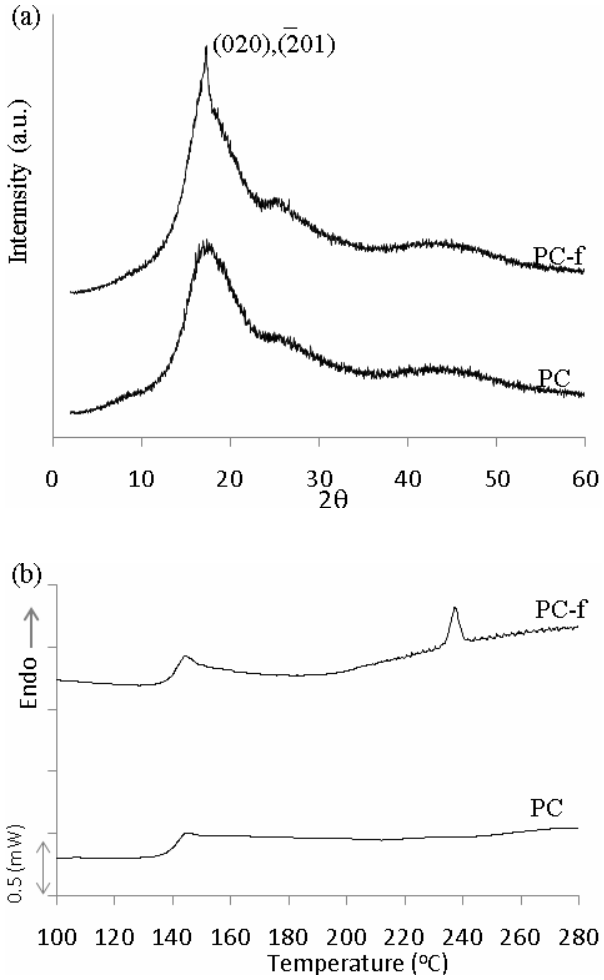

Figure 4. (a)WAXS spectra and (b) DSC heating curves of PC-f with a relative density of 0.38 and the unfoamed PC.

Enhanced thermal stability

The TGA and respective DTG thermograms of the unfoamed and foamed polycarbonate (PC and PC-f respectively) were obtained under both nitrogen and air atmospheres. For instance, PC showed a characteristic one-step decomposition process with an onset temperature at 1 wt% loss of 388 ºC and a T_{max}, defined as the temperature at maximum mass loss rate in the DTG curve, of 430 ºC. It is well known that the main degradation pathways of polycarbonate can be classified into two categories: chain scission of isopropylidene bonds and hydrolysis/alcoholysis of carbonate bonds, including rearrangements of some carbonate bonds like decarboxylation or cross-linking upon heating, ultimately resulting in CO_2, H_2O and char [24].

The corresponding DTG thermogram suggested that two events could be occurring at different rates due to the shoulder observed in Figure 5(a), related to a smaller quantity of material undergoing the degradation process at that temperature. The PC-f samples showed a similar one-step decomposition, where was a delay corresponding to the beginning of the process for a 1 wt% loss of about 34 ºC and of 55 ºC for a 5 wt% loss when compared to the unfoamed material for a PC-f with a relative intensity of 0.38. The DTG curve showed a T_{max} shifted 70 ºC higher than for the unfoamed PC, however the degradation process occurred faster for the PC-f compared to the unfoamed material. The delay during the beginning of the degradation process was attributed to the material's cellular structure, which acted as an improved thermal insulator, inhibiting heat transfer at the beginning of the thermal decomposition process. In general the process was delayed while decreasing the relative density due to the thermal insulator explained above and the presence of crystalline structure confirmed by WAXS and DSC.

The thermal decomposition of PC in air occurred in three stages, as can be seen in Figure 5(b). The first stage corresponded to the thermo-oxidative decomposition of PC in air. The degradation process started with the chain scission of the isopropylidene bonds, including alcoholysis and hydrolysis of the carbonate bonds, similar to that under nitrogen atmosphere. The second stage (stage II) of the degradation process presented a slighter mass loss slope than the first main stage of degradation and had the shortest period of time of the three main degradation stages. This stage was attributed to the decomposition of the remaining polymer that was kept protected from burning due to the char layer formed during stage I, as well as the degradation of part of that previous char layer. Stage III was attributed to char oxidation produced in the previous stages. No solid residues were obtained after 1000 ºC, indicating a complete thermo-oxidative decomposition process of polycarbonate.

PC-f under air presented a shift in the temperature corresponding to the first decomposition stage towards higher values when compared to the unfoamed PC; for instance, the 1 and 5 wt% loss temperatures were delayed in 25 and 30 ºC, respectively. The DTG showed how the degradation process occurred faster than for the unfoamed PC, with a T_{max} shift of 16 ºC (see Figure 5(b)). The delay observed during the beginning of the degradation process was once again attributed to the cellular structure, which acted as a thermal insulator within the material, inhibiting heat transfer at the beginning of the thermal decomposition process, and to the presence of the crystalline phase [25].

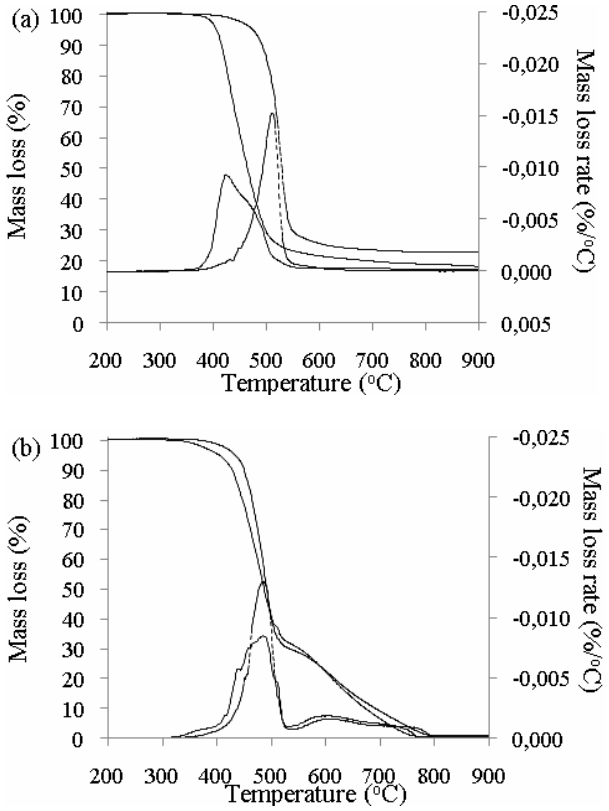

Figure 5. TGA and DTG thermograms of the unfoamed PC (continuous line) and foamed polycarbonate (PC-f, relative intensity: 0.38, dashed line), (a) under nitrogen and (b) under air atmosphere.

Conclusions

Polycarbonate foams were prepared and characterized in terms of their cellular structure characteristics. The study of the desorption kinetics of CO_2 out of PC showed similar values of the maximum CO_2 concentration dissolved into the material compared to the values found in the literature. The small difference of those values could be related to the degree of crystallinity present in the material.

The saturation/foaming temperature had a large effect on the morphology of the foams, with foams displaying smaller cell sizes with decreasing this temperature. This was attributed to a fast cooling of the polymer, which stopped foam growth once the glass transition temperature was reached, and due to the presence of crystalline structures confirmed by WAXS and DSC measurements. In addition to the saturation temperature, other foaming parameters that resulted relevant for the degree of achieved crystallinity were the pressure and the time at saturation conditions, which promoted the formation and perfection of crystals. The simultaneous presence of the cellular structure and crystals enhanced the thermal stability of polycarbonate, which increased while decreasing the relative density of the samples.

Acknowledgements

The authors would like to acknowledge the Spanish Ministry of Economy and Competitiveness for the financial support of project MAT2011-26410.

References

1. A. Landrock, Handbook of Plastic Foams, Noyes, New Jersey (1995).
2. M.S. Yun, W.I. Lee, *Comp. Sci.Tech,* **68**, 202 (2008).
3. V. Kumar, J. Weller, *J. Eng. Industry* **116**, 413 (1994).
4. L.J. Lee, C. Zeng, X. Cao, X. Han, J. Shen, G. Xu, *Comp. Sci. Tech.* **65**, 2344 (2005).
5. A.I. Cooper, *J. Mater. Chem.* **10**, 207 (2000).
6. K. Goren, L. Chen, L.S. Schadler, R. Ozisik, *J. Superc. Fluids* **51**, 420 (2010).
7. M. Antunes, V. Realinho, J.I. Velasco, *J. Nanomater*, Article ID 306384 (2010).
8. X. Hu, A. J. Lesser, *Polymer* **45**, 2333 (2004).
9. E. Turska, H. Janeczek, *Polymer* **20**, 855 (1979).
10. J.M. Jonza, R.S. Porter, *J. Polym. Sci. Part B: Polymer Physics* **24**, 2459 (1986).
11. E. Laredo, M. Grimau, P. Barriola, A. Bello, A.J. Müller, *Polymer* **46**, 6532 (2005).
12. E. Beckman, R.S. Porter, *J. Polym. Sci. Part B: Polymer Physics* **25**, 1511 (1987).
13. T. Takahashi, K. Yonetake, K. Koyama, T. Kikuchi, *Macromol. Rapid Commun,* **24**, 763 (2003).
14. V.N. Bliznyuk, V.N. Singamaneni, R.L. Sanford, D. Chiappetta, B. Crooker, P.V. Shibaev, *Polymer* **47**, 3915 (2006).
15. G. Gedler, M. Antunes, V. Realinho, J.I. Velasco, *IOP Conference Series: Materials Science and Engineering* **31**, 012008 (2012).
16. J. Crank, The mathematics of diffusion, Oxford University Press, London (1956).
17. J. Brandrup, E.H. Immergut, Polymer Handbook, Wiley, New York, Ed. 2nd (1975).
18. G.L.A. Sims, K.C. Khunniteekool, *Cell Polym* **13**, 137 (1994).
19. L. Sorrentino, E. Di Maio, S. Iannace, *J. Applied Polym. Sci,* **116**, 27 (2010).
20. M. Tang, T.B. Du, Y.P. Chen, *J. Superc. Fluids* **28**, 207 (2004).
21. M. Tang, W.H. Huang, Y.P. Chen, *J. Chinese Institute of Chemical Engineers* **38**, 419 (2007).
22. R. Bonart, Makromol. Chem., **92**, 149 (1966).
23. Z. Fan, C. Shu, Y. Yu, V. Zaporojtchenko, F. Faupel, *Polym. Eng. Sci.* **46**, 729 (2006).
24. B.N. Jang, C.A. Wilkie, *Polym. Degrad. Stab,* **86**, 419 (2004).
25. G. Gedler, M. Antunes, V. Realinho, J.I. Velasco, *Polym. Degrad. Stab.,* **97**, 1297 (2012).

Key Words: Polycarbonate foams, Supercritical CO_2, Crystallinity microstructure.